ENGINEERING Agriculture

Engineering Journals

RESEARCH ARTICLE

2026 / Volume 13 / Issue 4 / 26679

Effect of split drip irrigation with limited water supply on soil water-salt dynamics and crop growth in a saline soil

Wei ZHU[1,2], Shiguo GU[2], Xin ZHANG[1], Rongjiang YAO (✉)[1]

1 State Key Laboratory of Soil and Sustainable Agriculture, Institute of Soil Science, Chinese Academy of Sciences, Nanjing 211135, China.

2 College of Civil and Architecture Engineering, Chuzhou University, Chuzhou 239000, China.

KEYWORDS

Mulched drip irrigation, Hydrus-2D, soil water, soil salt

HIGHLIGHTS

- Soil water content quickly increased under the single drip irrigation.
- The split drip irrigation could maintain soil water content in root zone.
- The split drip irrigation improved soil salt leaching.

Received August 29, 2025;
Accepted October 22, 2025.

Correspondence: rjyao@issas.ac.cn

GRAPHICAL ABSTRACT

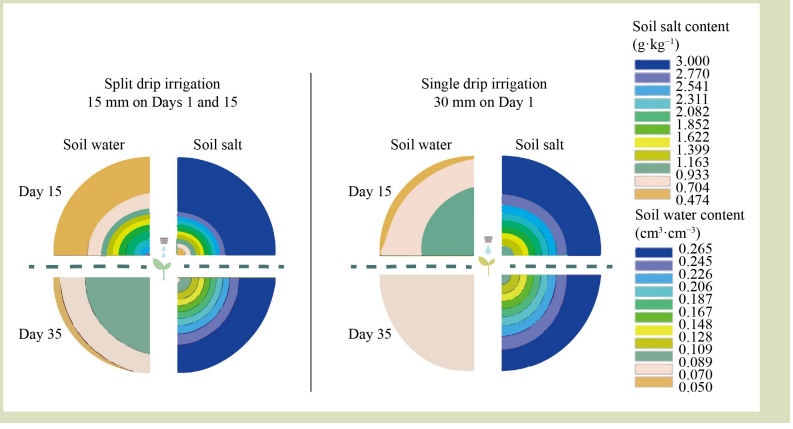

ABSTRACT

Mulched drip irrigation with appropriate strategies is recommended for effectively reclaiming saline soils in the Hetao Irrigation District of China. This study investigated soil water-salt dynamics and crop growth under different irrigation strategies through soil box experiments, scenario simulation experiments and field validation experiments, with particular focus on two drip irrigation strategies: single 30-mm irrigation and split irrigation (15 mm on Days 1 and 15). Hydrus-2D was used to simulate the distribution of water and salt. The results demonstrated that soil water content (SWC) fluctuated under mulched drip irrigation, with higher amounts near the drip emitter. The highest SWCs with the single and split irrigations were 0.22 and 0.19 $cm^3 \cdot cm^{-3}$, respectively. The split irrigation strategy better maintained SWC within the 0–25 cm depth range. Simulation experiments further revealed that increasing irrigation amounts to 40 or 50 mm effectively sustained soil water content, while producing salt leaching effects largely comparable to the 30-mm irrigation. The lower soil salinity (0.53 $g \cdot kg^{-1}$) was recorded with split irrigation. However, no significant differences in salinity were observed between the

tested mulched drip-irrigation strategies within the 0–15 cm soil depth. Field validation experiments demonstrated that split irrigation resulted in significantly greater plant height, stem diameter and leaf area index compared to the single irrigation at about 30 days after sowing. It was concluded that with a limited 30-mm irrigation, split drip irrigation effectively delays soil water depletion, performs better than a single drip irrigation by enhancing overall soil water content and promoting desalination, and thereby facilitating improved crop growth.

1 Introduction

Soil salinization is a significant challenge to irrigated agriculture in Hetao Irrigation District of China, where severe water scarcity affects a substantial portion of the region[1]. Enhancing irrigation water use efficiency is critical to address the escalating water demands in this area[2]. Thus, implementing effective irrigation techniques is essential to mitigate the adverse effects of both soil salinity and drought on crop growth. Additionally, the water and salt content within the root zone are key factors closely linked to the effectiveness of irrigation methods.

Mulched drip irrigation offers a viable alternative to current methods by optimizing water and nutrient use[3], through the application of water directly to the root zone and covering the soil with plastic film, thereby enhancing irrigation efficiency[4–6]. This technology has been widely adopted in arid and semiarid regions due to its effectiveness and financial feasibility, leading to water conservation and increased crop yields[7]. As leaching volume increased, salinity around the wetted zone of the drip emitter decreased[8]. In the dry regions of northwest China, an irrigation of 20–30 mm and a rate of 2.6 $L \cdot h^{-1}$ are recommended for effective salt leaching in silt loam soils[9]. Mulched drip irrigation mainly affects soil water and salinity in the top 30 cm of soil, with the salt tolerance threshold of the roots varying across growth stages. Soil water and salinity content during different phases impact the theoretical irrigation requirements[10,11]. For example, in Hetao Irrigation District, maize has a recommended soil salinity threshold of 0.3 $g \cdot kg^{-1}$ (salt per mass of soil)[12]. The area of soil desalination under mulch expands with increasing irrigation[13]. However, a standard irrigation of 30 mm often results in minor salt accumulation and reduced water availability 15 days after irrigation, a method that mostly used in this area, which highlights the need to refine irrigation strategies.

Regardless of the irrigation method, quantifying the temporal dynamics of water and salt, particularly during the seedling stage, remains challenging. Monitoring and simulating soil water and salinity are crucial for optimizing drip irrigation, especially in salt-affected soils in arid regions[14]. Standard methods for detecting soil water and salt content are often discontinuous and insensitive, and field experiments are time-consuming and costly[15]. Simulation models offer an alternative, provided they are tested and validated through field experiments. Studies have confirmed that models like Hydrus, SWAP and SWAT are effective tools for evaluating irrigation strategies across various crops and conditions[16–18]. Hydrus-2D, in particular, is widely used to simulate the movement of water and salt in saline soils, accounting for boundary conditions, including film mulch, buried wood fiber layer and tillage method. For example, Hydrus-2D successfully modeled water and salt dynamics under a compound control system using film mulch and a buried wood fiber layer in saline soils[16]. It was also applied to assess soil salt dynamics in a drip-irrigated field using brackish water under mulch with variable head boundary conditions[19].

Mulched drip irrigation is a promising method for efficient water delivery, but understanding the distribution of salt and water in the root zone requires specific conditions, such as limited irrigation once or twice per month in undisturbed, homogenous soil. Also, normal flood irrigation, however, is inefficient, leading to water waste, nutrient leaching and groundwater pollution[20]. Research shows that precise drip irrigation and single irrigation events push soil salt and water to the edges of the wetting zone[21], while nutrients, particularly nitrate, remain confined within the wetted soil[22].

To counter this effect, a targeted irrigation strategy was developed to reduce vertical water movement rate based on controlled water application and specific conditions.

Generally, 30 mm of irrigation water is applied at sowing in Hetao Irrigation District, and rapid declines in soil water are observed following drip irrigation, with salt accumulating on the surface within 15 days. To address this, using the Hydrus-2D model and soil box experiments, scenario simulation experiments and field validation experiments, with particular focus on two drip irrigation strategies: single 30-mm irrigation and a split irrigation (15 mm on Days 1 and 15), we analyzed soil water-salt dynamics and crop growth under different strategies. The primary objectives of this study were to maintain root zone soil water while reducing salt accumulation, and to predict water and salt movement under future drip irrigation strategies using multiple water sources. We hypothesized that both single and split drip irrigation strategies would improve salt leaching and water retention capacity, with the split irrigation strategy expected to prolong the effective duration of water and salt regulation in the root zone while promoting crop growth.

2 Materials and methods

2.1 Sampling sites and sample analysis

The salt-affected soil used in this study was obtained from irrigated farmland in Hetao Irrigation District (40°49.4′ N, 106°54.7′ E). The samples were collected from the topsoil to 30 cm deep. This area is characterized by a high evaporation-to-precipitation ratio (> 15), limited precipitation (< 200 mm) and shallow saline groundwater (with an EC of ~5 dS·m^{-1} and a water table at ~1 m). The soil texture is silty clay loam.

Field capacity was measured using the ring method[23]. Cation exchange capacity was measured using the ammonium replacement method. Bulk density was calculated from the volume-mass relationship of soil samples taken with a soil corer. Soil particle size distribution was determined by the hydrometer method, soil water content was determined using the gravimetric method and soil salt content was measured using the water bath drying method. Soil water and salt contents in the soil box were measured 1, 7, 15, 25 and 35 days after irrigation. Soil volumetric water content was calculated from the measured gravimetric water content and corresponding soil bulk density. Table 1 shows the soil textural properties of the field within a plot area of 2 m × 2 m, from which soil samples were collected for box experiments.

2.2 Experimental design

2.2.1 Soil box experiments

The effects of mulched drip irrigation on the transport and redistribution of soil water and salt were examined using soil box experiments. The box was packed in 15 cm layers to a depth of 50 cm and had a width of 45 cm, with a bulk density of 1.4 g·cm^{-3}. Six boxes were used, divided into two treatments with three replicates each. Details are shown in Fig. 1(a). The vertical and horizontal axes were oriented downward and to the right, respectively. The coordinates (X, Y) given in cm represent the position relative to the origin (0, 0), both horizontally and vertically, with all directions considered positive. Sixteen points were selected to evaluate soil water and salt redistribution under drip irrigation (Fig. 1(b)). Corresponding pores were used for soil sampling and were filled with similar soil after sampling.

A syringe needle served as the drip emitter, positioned beneath the plastic mulch at coordinates (cm) of (15, 0) with a water bottle was used to control the drip discharge, which was kept constant at 0.8 L·h^{-1}. The soil box experiment included two drip irrigation patterns: a single irrigation of 30 mm and a split irrigation of 15 mm on Days 1 and 15. All the soil boxes were kept in a constant temperature laboratory at 25 °C at the Institute of Soil Science, Chinese Academy of Sciences, China. The experiments lasted 35 days from 1 July to 4 August 2024.

Table 1 Average soil properties from three soil samples (n = 3)

Field capacity (%)	Cation exchange capacity (cmol·kg^{-1})	Soil bulk density (g·cm^{-3})	Soil particle-size distributions (%)			Soil texture
			Sand	Silt	Clay	
23.4 ± 0.3	15.8 ± 0.2	1.5 ± 0.1	21.4	60.3	18.3	Silty clay loam

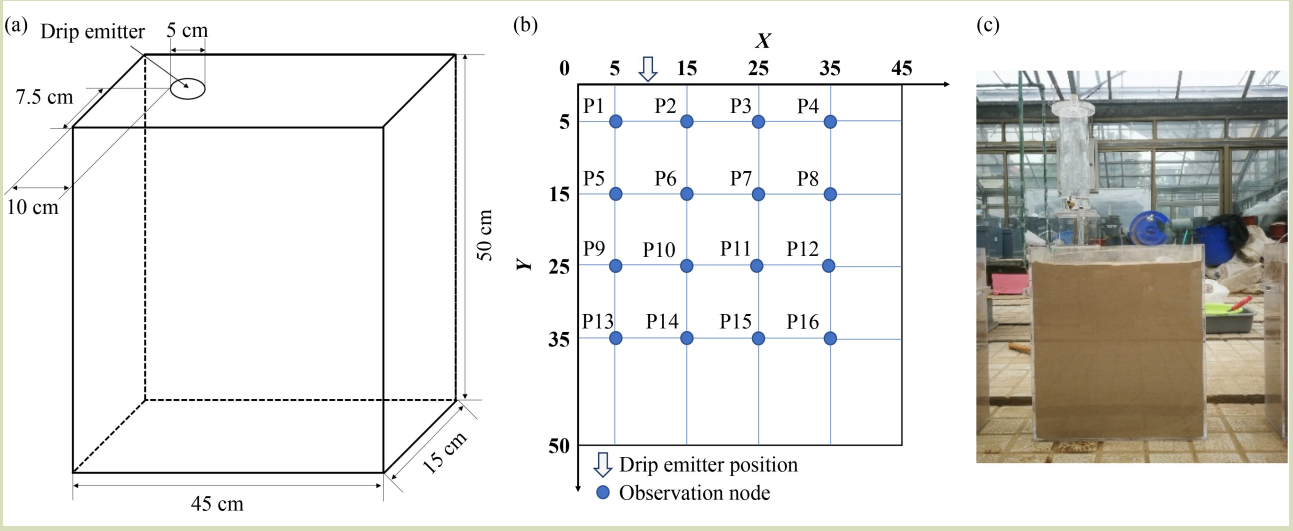

Fig. 1 Schematic diagram of the (a) soil column experiment, (b) observation points position, and (c) physical drawings of column experiment.

2.2.2 Field validation experiments

A field plot experiment was conducted to evaluate the effects of two drip irrigation methods. Each irrigation treatment was arranged in a randomized complete block design with five replicates. The experimental plots were established in a single field, with each plot measuring 7 m × 5 m (35 m^2), resulting in a total of 10 plots. Sunflower cv. Mengsha 531 was used and fertilizers were diammonium phosphate and urea, both sourced from local agricultural suppliers. Sunflower sowing was completed on 4 June 2025, and by the end of the observation period on 4 July, the plants were at the seedling stage. Irrigation water was supplied from a groundwater well which closed to the field, with quality parameters shown in Table 2.

The plastic film mulching configuration consisted of wide rows spaced of 90 cm and narrow rows of 40 cm, with plant spacing ranging from 45 to 50 cm. Drip irrigation tapes were laid concurrently with film mulching, and base fertilizers, diammonium phosphate (375 kg·ha^{-1}) and 45% potassium sulfate (150 kg·ha^{-1}) were applied. As this study focused on the first 30 days of the growth, no subsequent topdressing was applied. Also, to maintain the integrity of the early-stage irrigation treatments and the field experiment, no soil sampling was conducted in the irrigated plots. The evaluation of the irrigation methods on crop growth relied primarily on plant growth parameters, namely plant height, stem diameter and the leaf area index.

Seeds were sown when the temperature of the top 5-cm soil layer was higher than 14 °C. Two rows of sunflower were planted with a 30-cm spacing centered on 60 cm, with a narrow (20 cm) within-row spacing and wider (40 cm) between-row spacing. Fertilization was applied under the plastic film at a rate of 100 kg·ha^{-1} N. A plastic film mulch system was applied to 60 cm of the sunflower rows. The layout of the reference with only film mulch treatment was failed with limited yield, because seed germination was depressed from the high soil salt concentration during the early growth stage.

2.2.3 Scenario simulation experiments

Due to the shortage of irrigation water in Hetao Irrigation District, the 30-mm irrigation used was selected based on

Table 2 Water quality for irrigation (mg·L^{-1})

Ca^{2+}	Mg^{2+}	K^+ and Na^+	HCO_3^-	SO_4^{2-}	Cl^-	CO_3^{2-}	Total salt concentration
203 ± 54	121 ± 45	413 ± 192	509 ± 156	821 ± 362	396 ± 161	Not detected	2460 ± 729

water-saving irrigation requirements and the actual irrigation amount used from sowing to seedling emergence in production practices. Considering the potential future use of multiple water sources, scenario simulations were conducted to further investigate the characteristics of water and salt dynamics under increased irrigation volumes and split irrigation (Table 3).

2.3 Model description

Hydrus-2D was used to simulate the continuous dynamics of soil water and salt changes, leveraging its advantages, including non-interference, lack of time delay and the ability to model both horizontal and vertical variations of soil water and salt[24]. Water flow and solute transport were calculated using this model as (more details are provided in the Supplementary Material):

$$\frac{\partial \theta}{\partial t} = \frac{\partial}{\partial x}\left[K(h)\frac{\partial h}{\partial x}\right] + \frac{\partial}{\partial z}\left[K(h)\frac{\partial h}{\partial z}\right] + \frac{\partial K(h)}{\partial x} - \mathrm{S} \qquad (1)$$

where, θ is the volumetric water content of the soil ($cm^3 \cdot cm^{-3}$), t is the time (d), x is the horizontal axis (cm), $K(h)$ is the hydraulic conductivity ($cm \cdot d^{-1}$), h is the pressure head (cm), z is the vertical coordinate (cm) with positive upwards and S is the sink term accounting for water uptake by plant roots ($cm^3 \cdot cm^{-3} \cdot d^{-1}$), which was set to 0 for this study.

The general form of equation for soil salt migration in unsaturated soils as:

$$\frac{\partial(\theta C)}{\partial t} = \frac{\partial}{\partial x}\left[\theta D\frac{\partial C}{\partial x}\right] + \frac{\partial}{\partial z}\left[\theta D\frac{\partial C}{\partial z}\right] + \frac{\partial}{\partial z}(q_w C) \qquad (2)$$

where, C is the solute concentration in soil ($g \cdot cm^{-3}$), D is the dispersion coefficient ($cm^2 \cdot d^{-1}$) and q_w is the water flux ($cm \cdot d^{-1}$).

Soil hydraulic and transport parameters are shown in Table 4 and Table 5, respectively. At the beginning of the experiment, soil samples were collected for laboratory measurements of residual water content, saturated hydraulic conductivity and saturated water content, which were tested using a cutting ring method[23]. The parameters α, n and l were determined through inverse parameter estimation in Hydrus-2D. Parameter inversion was primarily performed by simulating and fitting parameters using measured hydraulic parameters and soil water-salt content data.

2.4 Initial and boundary conditions used in Hydrus-2D

To analyze the redistribution of soil water and salt in the horizontal and vertical directions (45 cm long and 50 cm deep),

Table 3 Irrigation amounts (mm) and timing used in the irrigation simulation experiment

Total irrigation	Day 1	Day 7	Day 15
40	15	10	15
50	15	20	15

Table 4 Average soil properties the top 50 cm (n = 3)

θr ($cm^3 \cdot cm^{-3}$)	θs ($cm^3 \cdot cm^{-3}$)	α (cm^{-1})	n	Ks ($cm \cdot d^{-1}$)	l
0.0466	0.380	0.0147	1.47	23.7	0.5

Note: θr, residual water content; θs, saturated water content; Alpha, reciprocal value of air-entry pressure; n, the smoothness of pore size distribution; Ks, saturated hydraulic conductivity; l, the tortuosity parameter in the conductivity function.

Table 5 Solute transport parameters

DisperL (cm)	DisperT (cm)	Frac	ThImob	DfiW ($cm^2 \cdot d^{-1}$)	DifG ($cm^2 \cdot d^{-1}$)
4.2	0.3	1	0	0.018	0

Note: DisperL, the longitudinal dispersivity; DisperT, the transverse dispersivity; Frac, it is 1 when equilibrium transport is considered; ThImob, immobile water content; DfiW, molecular diffusion coefficient in free water; and DfiG, molecular diffusion coefficient in soil air.

without disturbing the soil, Hydrus-2D was applied. The initial measured values for soil water content and salt concentration were 0.05 $cm^3 \cdot cm^{-3}$ and 3.00 $g \cdot kg^{-1}$, respectively. A time-variable flux boundary condition was specified at the emitter to represent drip irrigation, set to 5 cm for this study.

2.5 Statistical analysis

Data analysis was performed using Microsoft Excel 2016, and graphs were created using Origin (Version 9.0; Origin Lab Corporation, MA, USA). The significance of differences ($p \leqslant 0.05$) was tested using SPSS Statistics 27.0 (IBM Corp., Armonk, NY, USA). To compare the simulation results with the measured values, the root mean square error (RMSE) and Nash-Sutcliffe modeling efficiency (NSE) were calculated as:

$$\mathrm{RMSE} = \sqrt{\frac{1}{n}\sum_{i=1}^{n}(S_i - M_i)^2} \tag{3}$$

$$\mathrm{NSE} = 1 - \sum_{i=1}^{n}(M_i - S_i)^2 \Big/ \sum_{i=1}^{n}(M_i - M)^2 \tag{4}$$

where, S_i and M_i are the simulated and measured values, respectively, M is the mean values of measured and n is the number of data points.

The simulations were more accurate when the RMSE and NSE are closer to 0 and 1, respectively.

3 Results

3.1 Soil water dynamics under two drip irrigation strategies

3.1.1 Soil water dynamics with 30-mm limited drip irrigation

The dynamics of soil water within the top 50 cm of soil differed between the two strategies. There was a decreasing trend at various points, strongly influenced by the irrigation methods. A significant increase in soil water content was observed with the single irrigation (Fig. 2). The single irrigation resulted in the highest soil water content at P1 and P2, with values of 0.22 and 0.20 $cm^3 \cdot cm^{-3}$, respectively (Fig. 2(a)), which were higher than those in the split irrigation, where P1 and P2 had values of 0.18 and 0.16 $cm^3 \cdot cm^{-3}$, respectively. However, two peaks in soil water content were observed during the split irrigation, which effectively controlled soil water decline (Fig. 2(e)). The

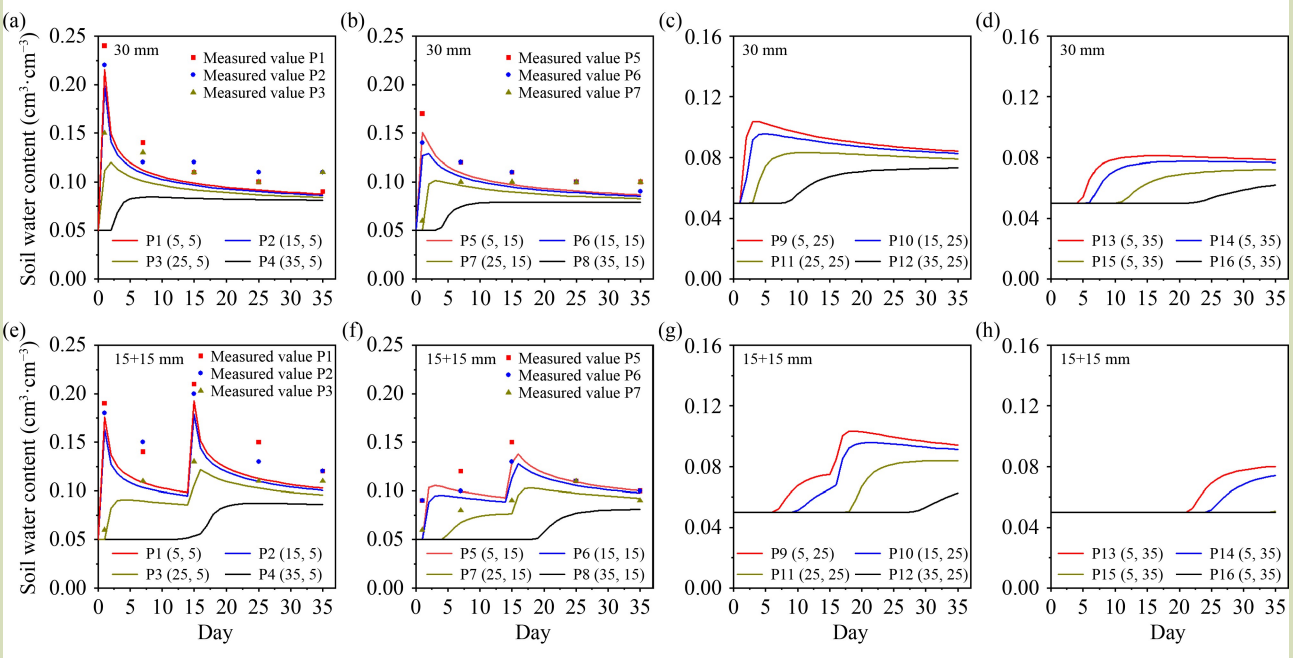

Fig. 2 Soil water content as a function of time for the various observation points (P) for the single drip irrigation (a–d), and split drip irrigation (e–h), respectively. Measured values of water content are plotted as symbols and are shown for P1–P3 and P5–P7. (a, e) P1–P4; (b, f) P5–P8; (c, g) P9–P12; (d, h) P13–P16.

split irrigation also significantly improved soil water content at P1 and P2. A significant difference ($p < 0.05$) was observed between the single and split irrigation strategies during the second irrigation period at P1, P2 and P3. There was a considerable lag in response to drip irrigation, and the duration of the lag varied across different positions. With the single irrigation, the minimum and maximum lag times were at P7 and P16, with 2 and 20 days, respectively (Fig. 2(b,d). In the case of split irrigation, the minimum and maximum lag times were at P3 and P16, with 2 and 24 days, respectively (Fig. 2(e,h)).

3.1.2 Soil water dynamics with 40- and 50-mm limited drip irrigation

Increasing irrigation volume and adjusting irrigation frequency can effectively enhance and maintain soil water. Both the 40- and 50-mm total irrigation amounts significantly and rapidly increased soil water content. After the first irrigation, the soil water content at positions P1 and P2 reached about 0.20 $cm^3 \cdot cm^{-3}$ (Fig. 3(a,e)). Following the second and third irrigations, soil water content at these positions further increased, peaking at 0.25 $cm^3 \cdot cm^{-3}$ (Fig. 3(a,e)). At other positions, similar to the 30-mm irrigation treatment, a lag response was observed. Positions P3, P5 and P6 responded to all three irrigation events (Fig. 3(b,f)), whereas positions P9, P10 and P11 had only a single noticeable increase in soil water (Fig. 3(c,g)). Additionally, at 35 cm deep, water infiltration was still evident with the 50-mm irrigation, whereas the 40-mm irrigation resulted in no infiltration, similar to the 30-mm irrigation (Fig. 3(d,h)). These results demonstrate that increasing both irrigation volume and frequency can more effectively enhance and sustain soil water content in the upper soil layer.

3.2 Soil salt dynamics under two drip irrigation strategies

3.2.1 Soil salt dynamics with 30-mm limited irrigation

With the single irrigation, soil salt concentration significantly declined within a horizontal radius of 5 cm, as shown by P1 and P2 (Fig. 4(a)). This downward trend mainly occurred during the first 2 days after irrigation (Fig. 4(a)). The two lowest soil salt concentrations, 0.50 and 0.57 $g \cdot kg^{-1}$ for P1 and P2, respectively, were recorded on Day 1 following the initial irrigation. The declining trend mostly occurred over the first 2 days (Fig. 4(a,b)). A slight upward trend was observed due to

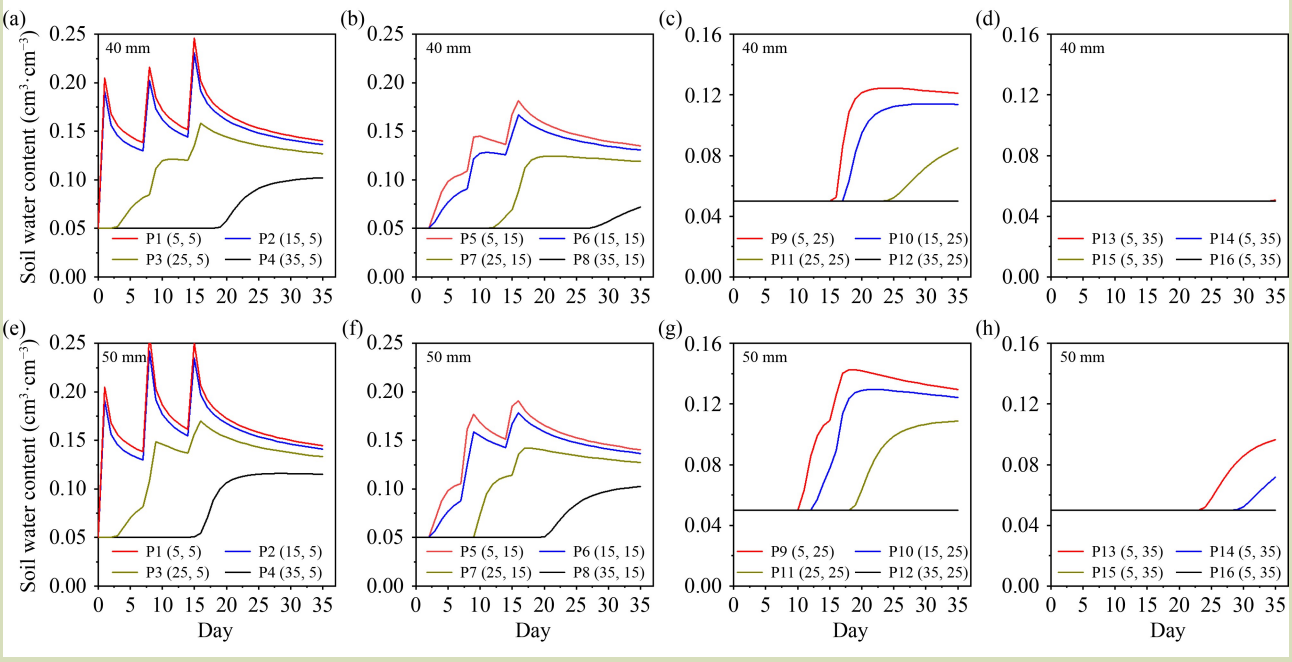

Fig. 3 Soil water content as a function of time for the various observation points (P) for irrigation amounts with 40-mm (a–d) and 50-mm (e–h), respectively. (a, e) P1–P4; (b, f) P5–P8; (c, g) P9–P12; (d, h) P13–P16.

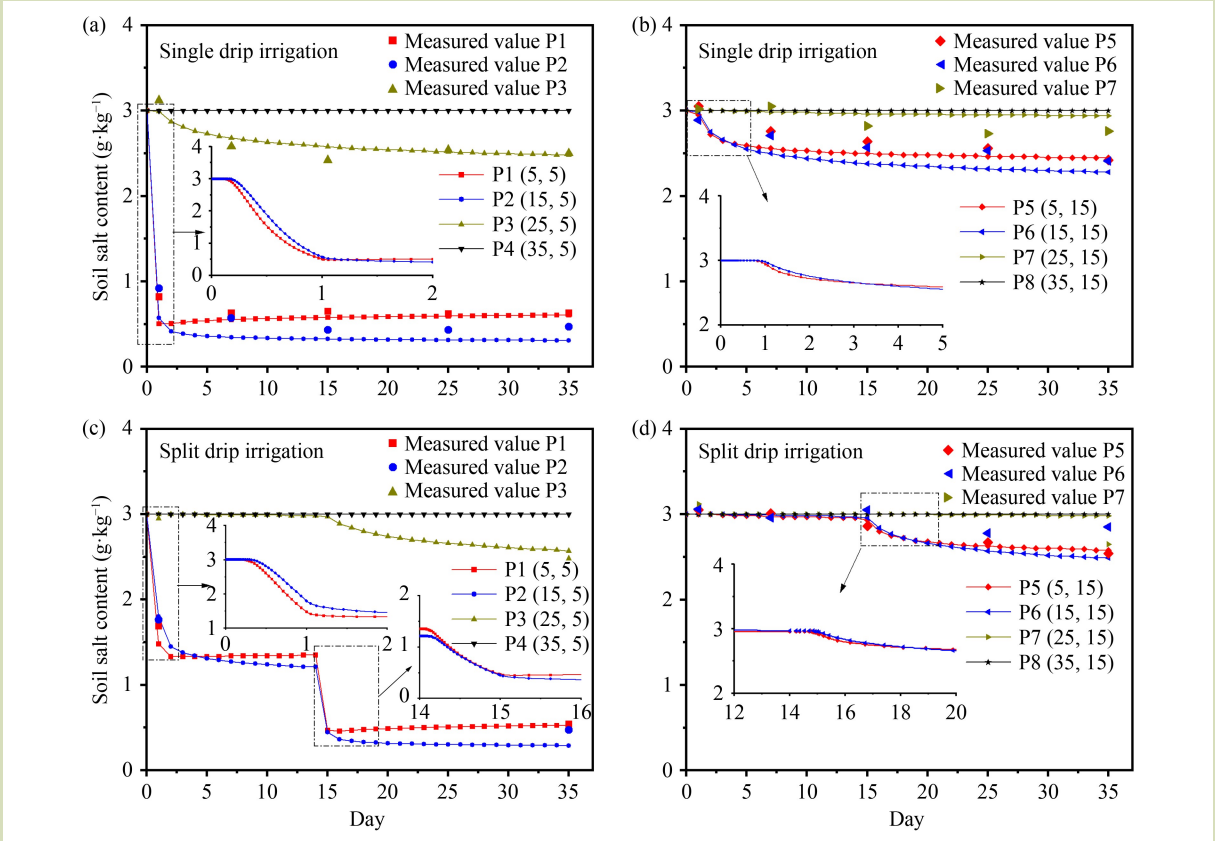

Fig. 4 Soil salt concentration as a function of time for the various observation points (P) for two drip irrigation strategies. Easured values of water content are plotted as symbols and are shown for P1–P3 (a, c) and P5–P7 (b, d). (a) P1–P4 under single drip irrigation; (b) P5–P8 under single drip irrigation; (c) P1–P4 under split drip irrigation; (d) P5–P8 under split drip irrigation.

mulch. The final soil salt concentration was 2.48 g·kg^{-1}, indicating moderately saline soil, and a steady decline in P3 was observed starting from 3 days after irrigation. At P5 and P6, which were at the same depth (Y = 15 cm) as P3, the soil salt concentration slightly decreased, reaching final values of 2.45 and 2.28 g·kg^{-1} in P5 and P6, respectively. The downward trend also occurred 2 days after irrigation, but the rate of decline was smaller than that of P1 and P2. Data analysis revealed a significant difference ($p < 0.05$) between single and split irrigation in the 0–15 day period for P1, P2, P5 and P6, with no significant difference after 25 days.

The volume and frequency of irrigation were key factors regulating soil salt changes with split irrigation (Fig. 4(c,d)). Two periods of changes in soil salt concentrations were observed in P1 and P2 at Y = 5 cm during separate irrigation (Fig. 4(c)), with the absolute difference during the first period being greater than that of the second (insets in Fig. 4(c)). During the first period, the salt concentrations were 1.52 and 1.20 g·kg^{-1} in P1 and P2, respectively, whereas during the second period, they were 0.88 and 0.76 g·kg^{-1} in P1 and P2, respectively. From the second irrigation onwards, the soil salt concentration in P3 decreased, with the final salt concentration reaching 2.57 g·kg^{-1}. In P5 and P6, which were comparable to the single irrigation, changes occurred during the second irrigation but were delayed by ~15 days. The lowest soil salt concentrations in P5 and P6 were 2.58 and 2.49 g·kg^{-1}, respectively, which were close to the value of P3.

3.2.2 Soil salt dynamics with 40- and 50-mm limited irrigation

Every irrigation event significantly reduced soil salt concentration within a 5 cm horizontal radius, particularly at positions P1, P2, P5 and P6 (Fig. 5(a,b,e,f)). Specifically, soil

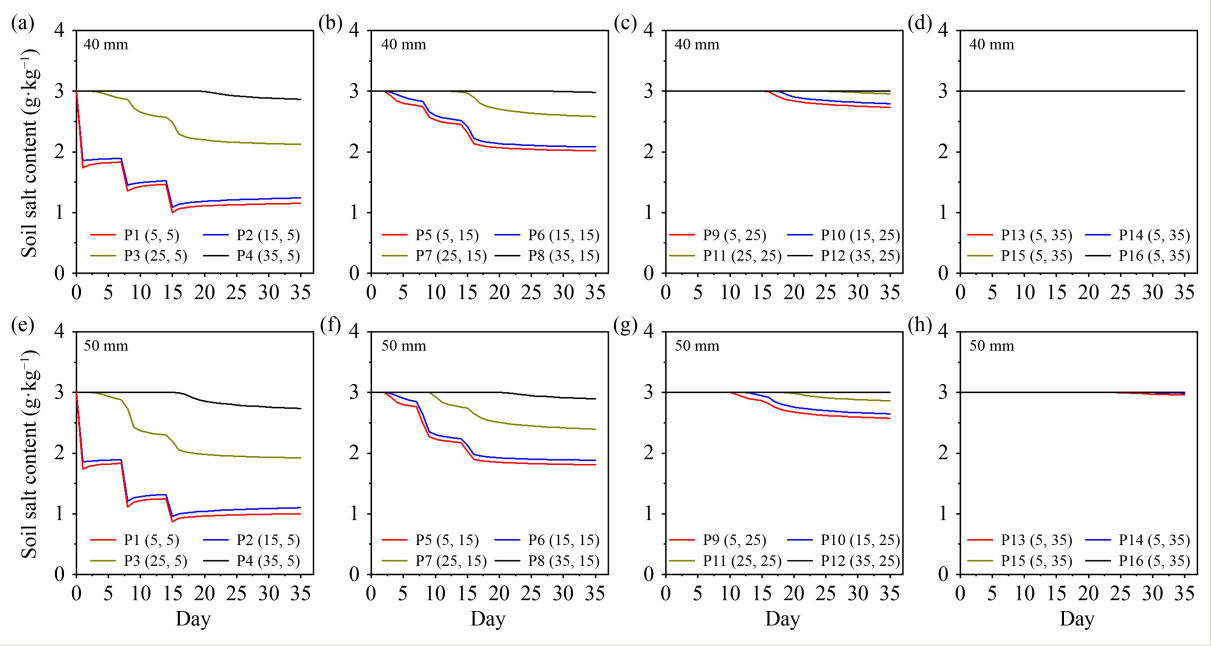

Fig. 5 Soil salt concentration as a function of time for the various observation points (P) for irrigation amounts with 40 mm (a–d) and 50 mm (e–h), respectively. (a) and (e), P1–P4; (b) and (f), P5–P8; (c) and (g), P9–P12; (d) and (h), P13–P16.

salt concentration at P1 and P2 decreased to 1.80 g·kg^{-1} after the first irrigation. With 40-mm total irrigation, it further declined to 1.40 and 1.00 g·kg^{-1} after the second and third irrigations, respectively, whereas with 50-mm total irrigation, it decreased to 1.20 and 0.90 g·kg^{-1} after the second and third irrigations, respectively (Fig. 5(a,e)). Within the top 15 cm depth, the leaching effects on soil salinity at the same positions were generally similar between the 40- and 50-mm irrigation amounts, with no significant differences observed (Fig. 5(b,f)). However, some variations in salt leaching were noted at positions P9, P10, and P11 (Fig. 5(c,g)). In deeper soil layers (35 cm), there was essentially no reduction in soil salt concentration (Fig. 5(d,h)). Overall, increasing the irrigation volume and frequency did not significantly enhance the final leaching effect on surface soil salinity. Instead, the main impact of higher irrigation amounts and frequency was observed in the leaching of salts in deeper soil layers.

3.3 Soil water and salt profile with 30-mm limited irrigation

3.3.1 Soil water profile

Soil water content rose immediately after the single irrigation on Day 1, with horizontal diffusion extending 25 cm and vertical diffusion reaching 20 cm, both aligning with the designed depth of the irrigation water (Fig. 6(a)). The water infiltration depth reached 35 cm by Day 7 (Fig. 6(b)). On subsequent days (15, 25 and 35) the infiltration depths were about 38, 40 and 45 cm, respectively (Fig. 6(c–e)). However, the soil water content at all points remained below 0.10 cm^3·cm^{-3}. Overall, the single irrigation achieved significant soil coverage, with horizontal diffusion exceeding vertical diffusion.

The horizontal and vertical diffusion distances were both about 25 cm (Fig. 6(f)), and 7 days after the first irrigation, they were 30 and 23 cm, respectively (Fig. 6(g)). The second irrigation increased soil water content within a range of 15 cm (Fig. 6(h)). Also the second irrigation primarily affected soil water content to a depth of 35 cm (Fig. 6(i,j)). Overall, split irrigation helped maintain surface soil water content. However, the water diffusion zone was smaller than with the single irrigation, despite the horizontal and vertical diffusion distances being similar.

3.3.2 Soil salt profile

The surface soil salt concentration rapidly decreased after the

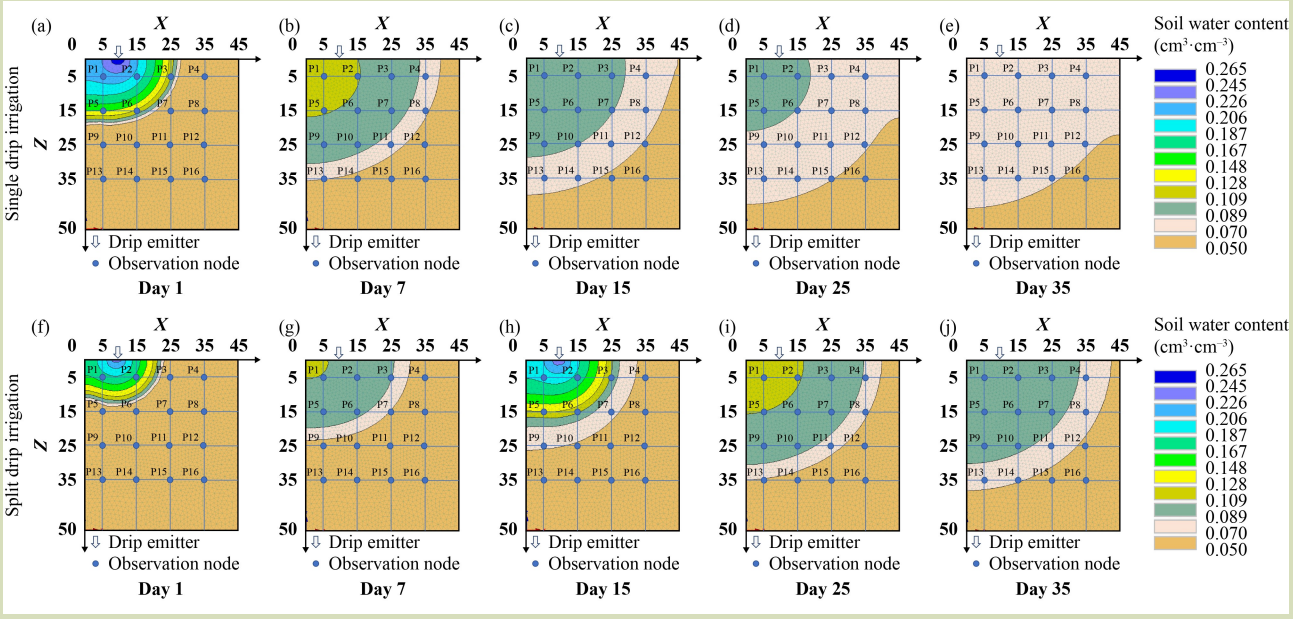

Fig. 6 Soil water profile distribution under two drip irrigation strategies after different days. The coordinates (*X*, *Z*) in cm represent the position relative to the origin (0, 0) both horizontally and vertically, with all directions set to positive. Sixteen points (P1–P16) were placed for soil sampling. (a–e) Single drip irrigation; (f–j) split drip irrigation; (a, f) Day 1; (b, g) Day 7; (c, h) Day 15; (d, i) Day 25; (e, j) Day 35.

single irrigation, and within the coordinate (cm) range of (0, 0) to (30, 25), soil salt was redistributed. The closer the soil was to the dripper, the lower the salt content (Fig. 7(a–e)). Soil salinity gradually increased near the drip emitter after irrigation stopped whereas salt concentrations in other areas remained largely unchanged (Fig. 7(a–e)). The minimum value range was typically within a 5 cm radius (Fig. 7(c–e)), and it progressively formed a semicircle around the center of the drip emitter. The desalting rate could reach 50% within the coordinate (cm) range of (0, 0) to (10, 20), with soil salt concentration dropping to below 1.50 g·kg^{-1}.

Split irrigation resulted in twice the amount of soil salt leaching, particularly within the coordinate (cm) range of (5, 0) to (15, 0), P2–P1. The lowest soil salt concentration, 0.46 g·kg^{-1}, was observed after the second irrigation, and this value was similar to that in the single irrigation. The soil salt distribution was altered in a smaller region compared to the single irrigation (Fig. 7(f,g)). However, the soil salt concentration near the drip emitter was lower than in the single irrigation, and the salt leaching region was also smaller (Fig. 7(h–j)).

3.4 Plant growth with 30-mm limited irrigation

Plant height, stem diameter and leaf area index under the two irrigation strategies indicated that split irrigation effectively promoted crop growth (Fig. 8). After irrigation, the single irrigation did not significantly improve plant growth. By Day 30, the split irrigation resulted in significantly greater plant height and leaf area index compared to the single irrigation, with average values of 49.2 cm and 1.7 compared to 41.1 cm and 1.2, respectively (Fig. 8(a,c)). There was, however, no significant difference was observed in stem diameter (Fig. 8(b)).

4 Discussion

4.1 Model evaluation

A fair level of agreement was found between the simulated and measured values (Table S1) for soil water (Fig. 2(a,b,e,f)) and salt (Fig. 4) with both irrigation strategies. Overall, the simulations were consistent for both soil water and salt, with the Hydrus-2D model performing better for soil water than for soil salt (Table S1). These differences may stem from the fact

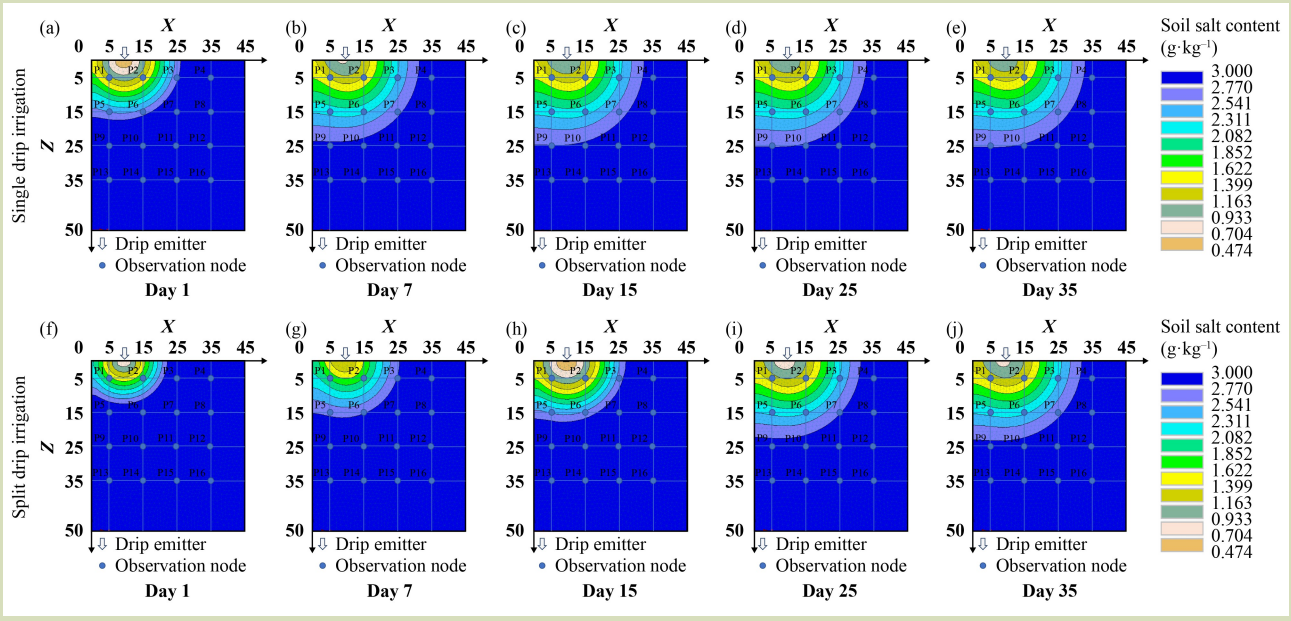

Fig. 7 Soil salt profile distribution under two drip irrigation strategies after different days. The coordinates (*X*, *Z*) given in cm represent the position relative to the origin (0, 0) both horizontally and vertically, with all directions set to positive. Sixteen points (P1–P16) were placed for soil sampling. (a–e) Single drip irrigation; (f–j) split drip irrigation; (a, f) Day 1; (b, g) Day 7; (c, h) Day 15; (d, i) Day 25; (e, j) Day 35.

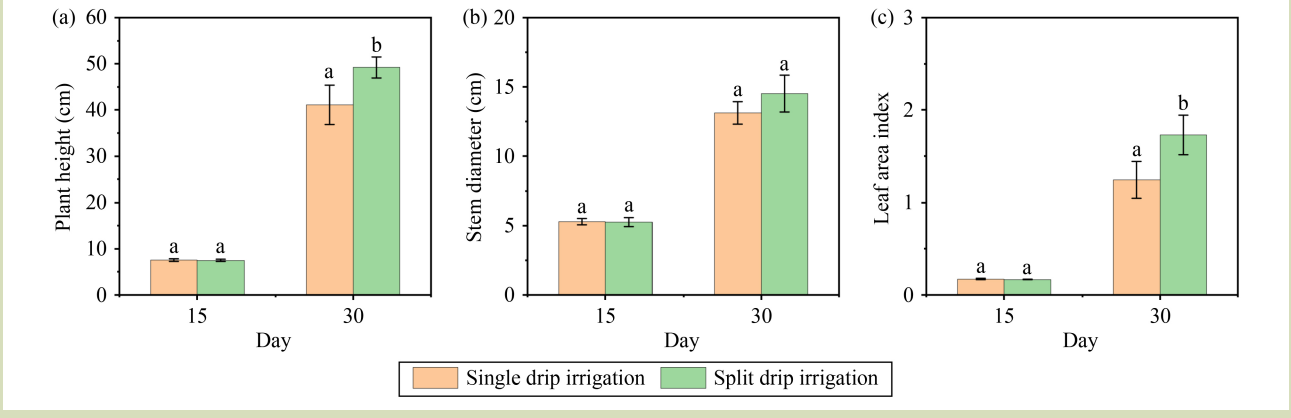

Fig. 8 Plant height (a), stem diameter (b), and leaf area index (c) under the two irrigation strategies.

that the initial distribution of soil water was more uniform than that of soil salt[25]. The RMSE and NSE values at different points, based on the measured and simulated data. The Hydrus-2D model effectively simulated the dynamics of soil water and salt, with RMSE ranging from 0.012 to 0.026 and NSE from −1.174 to 0.895 for soil water content, and RMSE from 0.012 to 0.026 and NSE from −1.174 to 0.895 for soil salt concentration with both single and split irrigation (Table S1). Numerous previous studies have confirmed the excellent capabilities of the Hydrus-2D model in explaining the dynamics of soil water and salt under various initial and boundary conditions[8,15,19]. Similarly, several investigations have validated the applicability of Hydrus model in Hetao Irrigation District, particularly regarding changes in soil water and salt content [26–28]. In the present study, soil water content varied consistently with irrigation schedules and frequency

(Figs. 2–4), and the film mulch system helped reduce soil evaporation. Also, environmental factors can significantly contribute to discrepancies between measured and simulated values[29], which may explain the differences between our results and those of other studies. In the present study, the soil box material and the boundary conditions of the inner wall contributed to less than optimal simulation. Nevertheless, Hydrus-2D is generally a suitable model for simulating soil water and salt dynamics in a mulched drip irrigation system[30].

4.2 Comparison of the two irrigation strategies

The soil water content at observation nodes near the bottom was lower than 0.09 $cm^3 \cdot cm^{-3}$ (Fig. 2), indicating that the single irrigation (30 mm) was primarily confined to a semicircle with a radius of 25 cm. This distribution could improve seed germination and meet the water requirements of seedlings[31,32]. During the first 15 days, most of the split irrigation water (15 + 15 mm) was concentrated within a smaller semicircle (radius < 25 cm), which indicates that the split irrigation has the potential to maintain irrigation water at the sowing zone without exacerbating soil salinization, its role aligns with previous studies on flood irrigation or winter irrigation[21,33]. The scenario simulation experiments showed that increasing the irrigation amount and frequency did not effectively enhance the deep infiltration depth, which remained confined to a semicircular area with a radius of 25 cm, however, it did increase the shallow soil water content and helped maintain its stability (Fig. 3). From this perspective, with water-saving irrigation strategies, a 30-mm irrigation can meet the needs of seed germination and seedling development. Practical application also confirmed that, in the first 15 days, there was no significant difference in plant growth between single and split irrigation. However, by Day 30, split irrigation significantly improved plant height and leaf area index but not stem diameter (Fig. 8). 30 Days later, there were no significant differences between the single irrigation and the split irrigation, because soil water retention depends primarily on the applied irrigation amount[34]. Also, split irrigation maintained surface soil water more effectively than the single irrigation (Fig. 6). The split irrigation facilitated two infiltration events, enhancing soil water content, and revealed that irrigation frequency determined irrigation efficiency[35], increasing the irrigation frequency while raising the irrigation volume maintained this effect (Fig. 3). The frequency of irrigation also affects the wetted radius and volume[36], which are influenced by irrigation interval, amount and rate[37]. Both single and split irrigation showed a significant infiltration delay, with the lag effect in deeper soil layers more pronounced with the split irrigation (Fig. 2), due to the limited quantity applied during the irrigation events[38]. However, this study found that the delay persisted even when the irrigation volume was increased by 10 and 20 mm. Therefore, the lag time correlates with the total irrigation volume and frequency: the greater the total volume and the higher the frequency, the shorter the lag time (Fig. 3). The single irrigation immediately increased soil water content in the root zone (Fig. 2), and the wetting front reached a depth of 35 cm, exceeding the expected depth of 30 cm, which was followed by a soil water content decline (Fig. 6(a–e)), for the water potential difference between the wetted area and the surrounding dry soil[39]. In contrast, the split irrigation helped reduce this water potential difference within a certain area by allowing for split infiltration processes (Fig. 6(f–j)). The amount of irrigation and emitter location directly influenced the region where soil water content varied the most[40], that is, with coordinate (cm) range (X, Y) < (25, 15) in the present study. In the field experiment, the main factors contributing to the decline in soil water content were soil evaporation and crop water absorption[41,42]. Mulch and infiltration can also contribute to changes in soil water content[43]. Previous studies have demonstrated that soil water migration and distribution were crucial for determining irrigation amounts and management[44]. With two stages, split irrigation can efficiently reduce the infiltration rate in the vertical direction, extend the period of high soil water content within the coordinate (cm) range of (X, Y) < (15, 25), and maintain this water content over both infiltration processes by reducing the water potential difference in this zone. In general, limited irrigation, applied once or twice a month in soil box experiments, such as the single irrigation of 30 mm or split irrigation of the same total amount (15 mm on Days 1 and 15 mm), can improve water use efficiency. Increasing the irrigation volume and frequency did not yield positive effects. Against the backdrop of water-saving irrigation in Hetao Irrigation District, split drip irrigation with a limited 30-mm total amount can effectively meet soil water requirements after sowing. Studies have also confirmed that drip irrigation within the root zone promotes seed germination and crop root growth[45], with this effect demonstrating a significant positive impact after the second irrigation event.

Soil salinity changes as a result of water infiltration[46], but the dynamics are primarily influenced by drip irrigation (e.g.,

amount, position, frequency, etc.)[47]. In the present study, the position of the drip emitter within 15 cm of the surface had a significant impact on salinity (Fig. 4). A noticeable drop in salinity was observed in the middle root zone (Fig. 7). The amount of irrigation has been found to determine the extent of soil salt leaching[48], however, in the present study the salt leaching effects with three irrigation volumes, 30, 40 and 50 mm, were not significant (Fig. 4 and Fig. 5). Considering the context of water-saving practices in Hetao Irrigation District and the practical requirements for salt control, increasing irrigation volume and frequency is not a particularly favored option[49]. With a total irrigation volume of 30 mm, both the single and split irrigation effectively reduced the soil salt concentration in the root zone. The study also demonstrated that soil salts would leach to a certain extent with a split irrigation. Irrigation frequency contributed to the efficiency of soil salt leaching due to the dual water infiltration processes[50], similarly, increasing the irrigation volume and frequency also gave comparable effects (Fig. 5). Also, soil texture significantly influences soil water infiltration and salt leaching processes. Generally, sandy soils have superior water infiltration capacity and salt leaching efficiency compared to fine-textured soils[51]. Additionally, agricultural practices such as deep plowing and buried wood fiber layer can effectively improve both water infiltration and salt leaching conditions[52,53]. Compared to the single irrigation, split irrigation resulted in two stages of soil salt leaching and a decreased final soil salt concentration within the 0–25 cm soil depth. Additionally, homogenous soil texture can improve salt leaching efficiency[54]. In the present study, there was a desalination zone with both split and the single irrigation, centered around the drip emitter. This zone can gradually spread horizontally and vertically[55], with desalination rates of 18.5%–22.9% in the present study.

After the first irrigation, the desalination ratios for the single irrigation and split irrigation were 82.0% and 45.3%, respectively (Table S2). These ratios fall within the salinity range suitable for seed germination[12], but there was no significant difference in the final desalination ratios between the two methods, with the single irrigation and split irrigation at 86.3% and 84.7%, respectively (Table S2). The analysis of the data did not indicate that split irrigation significantly enhanced salt reduction efficiency, as the effectiveness of salt leaching is mostly determined by the total irrigation amount applied[48]. However, after the second irrigation, soil water content was higher with the split irrigation than the single irrigation, especially in the coordinate (cm) range (5, 0) to (15, 0). Additionally, salt will move to the edges of the wetting zone for with irrigation and water applied at specific spatial locations[56]. Appropriate drip irrigation can maintain low salinity conditions in the root zone, which is conducive to seed germination and supports healthy seedling development[57]. This is also supported by a study showing that long-term frequent drip irrigation contributed to an 85.2% reduction in soil salinity in the top 40 cm of soil[58]. However, in the present study, the split irrigation strategy did not improve salt leaching within 0–15 cm around the drip emitter compared to the single irrigation. However, the salt reduction zone created by both methods can promote seed germination and crop root growth, based on the required water in the 0–30 cm soil depth and the frequently used irrigation amount during sowing.

5 Conclusions

In this study, the Hydrus-2D model demonstrated superior performance in simulating soil water compared to soil salt. A single drip irrigation immediately increased soil water content in the root zone, but this then declined due to the water potential difference between the wetting area and the dry soil. With both the single and split irrigation, soil water content increased more rapidly horizontally than vertically. However, the vertical infiltration depth was less in the split irrigation than in the single irrigation, leading to improved water use efficiency and maintaining a higher soil water content for a longer duration within the coordinate (cm) range of (X, Y) < (15, 25). Salt leaching correlated with the amount of irrigation, with two distinct processes of soil salt leaching observed with split irrigation. The final soil water content in the zone bounded by the coordinates (cm) of (5, 0) to (15, 0) was lower compared to the single irrigation method. Additionally, soil salinity led to the formation of a desalination zone centered around the drip emitter. The split irrigation tested has the potential to increase soil water content and enhance salt leaching near the drip emitter. This approach helps maintain soil water and salt contents within acceptable range, with no noticeable difference in its overall effect compared to the single irrigation, while also promoting crop growth. Increasing the irrigation amount to 40 or 50 mm, and its frequency can effectively maintain soil water, but there was no significant difference in salt leaching effectiveness between the strategies evaluated in this study. We also suggest that integrating other agronomic practices, such as deep plowing, could help in achieving more effective regulation of soil water and salt dynamics.

Supplementary materials

The online version of this article at https://doi.org/10.15302/J-FASE-2026679 contains supplementary materials (Text S1, Tables S1–S2).

Acknowledgements

This work was funded by National Key Research & Development Program of China (2021YFC3201201, 2021YFD1900602), National Natural Science Foundation of China (42507070, 32271720), and Chuzhou University Research Initiation Fund Project, China (2023qd44).

Compliance with ethics guidelines

Wei Zhu, Shiguo Gu, Xin Zhang, and Rongjiang Yao declare that they have no conflict of interest or financial conflicts to disclose. This article does not contain any studies with human or animal subjects performed by any of the authors.

REFERENCES

1. Wang X Q, Zhang H Y, Zhang Z Z, Zhang C P, Zhang K, Pang H C, Bell S M, Li Y Y, Chen J. Reinforced soil salinization with distance along the river: a case study of the Yellow River Basin. *Agricultural Water Management*, 2023, **279**: 108184
2. Li L Q, Jiang E H, Liu C, Xu C Y. How does top-down water unified allocation and regulation decelerate water utilization? Insights from the Yellow River, China. *Journal of Cleaner Production*, 2024, **447**: 141402
3. Chauhan S, Agrawal G, Kumar P, Chauhan A. Maximizing French bean yield, water use efficiency, and profitability using precision drip irrigation and organic mulching. *Plant and Soil*, 2025, **514**(2): 2495–2510
4. Che Z, Wang J, Li J S. Modeling strategies to balance salt leaching and nitrogen loss for drip irrigation with saline water in arid regions. *Agricultural Water Management*, 2022, **274**: 107943
5. Cohen B, Nitsan I, Ben-Noah I, Friedman S P. Simultaneous water uptake from shallow groundwater and drip irrigation: lysimeter experiments with ceramic cups. *Vadose Zone Journal*, 2025, **24**(2): e70012
6. Chen L, Wang R S, Xiao W, Wang L S. Optimizing irrigation and mulching strategies to improve root–water relations, water use efficiency, and yield in apple–soybean alley cropping systems on the Loess Plateau, China. *European Journal of Agronomy*, 2025, **168**: 127586
7. He P R, Li J G, Chen J, Chen D, Dai X P, Abdelghany A E, Qu Z Y. Impact of alternate irrigation with reclaimed water and saline water according to sunflower growth period on plant and grain development. *Field Crops Research*, 2025, **328**: 109948
8. Yang T, Šimůnek J, Mo M H, Mccullough-Sanden B, Shahrokhnia H, Cherchian S, Wu L S. Assessing salinity leaching efficiency in three soils by the HYDRUS-1D and -2D simulations. *Soil and Tillage Research*, 2019, **194**: 104342
9. Danierhan S, Shalamu A, Tumaerbai H, Guan D H. Effects of emitter discharge rates on soil salinity distribution and cotton (*Gossypium hirsutum* L.) yield under drip irrigation with plastic mulch in an arid region of Northwest China. *Journal of Arid Land*, 2013, **5**(1): 51–59
10. Zhang W Q, Dong A H, Liu F L, Niu W Q, Siddique K H M. Effect of film mulching on crop yield and water use efficiency in drip irrigation systems: a meta-analysis. *Soil and Tillage Research*, 2022, **221**: 105392
11. Shi H Y, Luo G P, Sutanudjaja E H, Hellwich O, Chen X, Ding J L, Wu S X, He X F, Chen C B, Ochege F U, Wang Y G, Ling Q, Kurban A, De Maeyer P, Van de Voorde T. Recent impacts of water management on dryland's salinization and degradation neutralization. *Science Bulletin*, 2023, **68**(24): 3240–3251
12. Ma J H, Yang S Q, Shi H B, Ding X H, Han W G. Irrigation schedule for maize based on soil moisture and salt content threshold in Hetao irrigation district. *Transactions of the Chinese Society of Agricultural Engineering*, 2014, **30**(11): 83–91 (in Chinese)
13. Qi Z J, Feng H, Zhao Y, Zhang T B, Yang A Z, Zhang Z X. Spatial distribution and simulation of soil moisture and salinity under mulched drip irrigation combined with tillage in an arid saline irrigation district, northwest China. *Agricultural Water Management*, 2018, **201**: 219–231
14. Šimůnek J, Brunetti G, Jacques D, van Genuchten M T, Šejna

M. Developments and applications of the HYDRUS computer software packages since 2016. *Vadose Zone Journal*, 2024, **23**(4): e20310

15. Phogat V, Cox J W, Kookana R S, Šimůnek J, Pitt T, Fleming N. Optimizing the riparian zone width near a river for controlling lateral migration of irrigation water and solutes. *Journal of Hydrology*, 2019, **570**: 637–646
16. Zhu W, Yang J S, Yao R J, Xie W P, Wang X P, Liu Y Q. Soil water-salt control and yield improvement under the effect of compound control in saline soil of the Yellow River Delta, China. *Agricultural Water Management*, 2022, **263**: 107455
17. de Melo M L A, de Jong van Lier Q, da Silva E H F M, de Almeida Pereira R A, van Dam J C, Heinen M, Marin F R. Field-scale modeling of root water uptake and crop growth in a tropical scenario. *Field Crops Research*, 2025, **322**: 109749
18. Wang R, Ren D Y, Jessen S, Xiong L, Jensen K H, Huang G H. Enhancing the representation of multi-level canal systems and reactive transport of nitrate in agro-hydrological modelling of arid irrigation districts. *Journal of Hydrology*, 2025, **658**: 133203
19. Zhang Y H, Li X Y, Šimůnek J, Shi H B, Chen N, Hu Q, Tian T. Evaluating soil salt dynamics in a field drip-irrigated with brackish water and leached with freshwater during different crop growth stages. *Agricultural Water Management*, 2021, **244**: 106601
20. Severini E, Magri M, Soana E, Bartoli M, Faggioli M, Celico F. Irrigation practices affect relationship between reduced nitrogen fertilizer use and improvement of river and groundwater chemistry. *Agricultural Water Management*, 2023, **289**: 108564
21. Dai J L, Cui Z P, Zhang Y J, Zhan L J, Nie J J, Cui J Q, Zhang D M, Xu S Z, Sun L, Chen B, Dong H Z. Enhancing stand establishment and yield formation of cotton with multiple drip irrigation during emergence in saline fields of Southern Xinjiang. *Field Crops Research*, 2024, **315**: 109482
22. Mohamadzade F, Gheysari M, Eshghizadeh H, Tabatabaei M S, Hoogenboom G. The effect of water and nitrogen on drip tape irrigated silage maize grown under arid conditions: experimental and simulations. *Agricultural Water Management*, 2022, **271**: 107821
23. Lu R K. Soil Argrochemistry Analysis Protocoes. Beijing: *China Agriculture Science Press*, 2000 (in Chinese)
24. Šimůnek J, van Genuchten M T, Šejna M. Development and applications of the HYDRUS and STANMOD software packages and related codes. *Vadose Zone Journal*, 2008, **7**(2): 587–600
25. Solat S, Alinazari F, Maroufpoor E, Shiri J, Karimi B. Modeling moisture bulb distribution on sloping lands: numerical and regression-based approaches. *Journal of Hydrology*, 2021, **601**: 126835
26. Nie W B, Dong S X, Li Y B, Ma X Y. Optimization of the border size on the irrigation district scale–Example of the Hetao irrigation district. *Agricultural Water Management*, 2021, **248**: 106768
27. Feng Z Z, Miao Q F, Shi H B, Feng W Y, Li X Y, Yan J W, Liu M H, Sun W, Dai L P, Liu J. Simulation of water balance and irrigation strategy of typical sand-layered farmland in the Hetao Irrigation District, China. *Agricultural Water Management*, 2023, **280**: 108236
28. Ramos T B, Liu M H, Paredes P, Shi H B, Feng Z Z, Lei H M, Pereira L S. Salts dynamics in maize irrigation in the Hetao plateau using static water table lysimeters and HYDRUS-1D with focus on the autumn leaching irrigation. *Agricultural Water Management*, 2023, **283**: 108306
29. Hu Q L, Zhao Y, Hu X L, Qi J, Suo L Z, Pan Y H, Song B, Chen X B. Effect of saline land reclamation by constructing the "Raised Field-Shallow Trench" pattern on agroecosystems in Yellow River Delta. *Agricultural Water Management*, 2022, **261**: 107345
30. Wang X F, Li Y, Biswas A, Sang H H, He J Q, Liu D L, Yu Q, Feng H, Siddique K H M. Modeling soil water and salt dynamics in cotton-sugarbeet intercropping and their monocultures with biochar application. *Soil and Tillage Research*, 2024, **240**: 106070
31. Gong X W, Qiu R J, Sun J S, Ge J K, Li Y B, Wang S S. Evapotranspiration and crop coefficient of tomato grown in a solar greenhouse under full and deficit irrigation. *Agricultural Water Management*, 2020, **235**: 106154
32. Liu H J, Yuan B Z, Hu X D, Yin C Y. Drip irrigation enhances water use efficiency without losses in cucumber yield and economic benefits in greenhouses in North China. *Irrigation Science*, 2022, **40**(2): 135–149
33. Li L, Liu H G, Gong P, Lin E, Bai Z T, Li P F, Wang C X, Li J. Multi-objective optimization of winter irrigation for cotton fields in salinized freeze-thaw areas. *European Journal of Agronomy*, 2023, **143**: 126715
34. Li Z P, Zhang F H, Ma Y Z, Wan S M, Han Y C, Chen G D, Lei Y P, Xiong S W, Mao T Y, Feng L, Wang G P, Li X F, Wang Z B, Zhi X Y, Jiao Y H, Xin M H, Li Y B, Yang B F. Rational optimization of irrigation regimes for drip-irrigated cotton fields without mulch can alleviate the problem of residual film contamination in arid zones. *Industrial Crops and Products*, 2024, **221**: 119430
35. Rix J P, Lo T H, Gholson D M, Pringle III H C, Spencer G D, Singh G. Effects of low-till parabolic subsoiling frequency and furrow irrigation frequency on maize in the Yazoo-Mississippi Delta. *Agricultural Water Management*, 2022, **274**: 107945
36. Cote C M, Bristow K L, Charlesworth P B, Cook F J, Thorburn P J. Analysis of soil wetting and solute transport in subsurface trickle irrigation. *Irrigation Science*, 2003, **22**(3–4): 143–156
37. Phogat V, Mahadevan M, Skewes M, Cox J W. Modelling soil water and salt dynamics under pulsed and continuous surface

drip irrigation of almond and implications of system design. *Irrigation Science*, 2012, **30**(4): 315–333

38. Wang Y J, Zhang Z T, Chen Y W, Fan S S, Chen H Y, Bai X Q, Yang N, Tang Z J, Qian L, Mao Z X, Zhang S Y, Chen J Y, Xiang Y Z. Correction of crop water deficit indicators based on time-lag effects for improved farmland water status assessment. *Agricultural Water Management*, 2025, **313**: 109480
39. Tirgarsoltani M, Bahrami H, Mokhtassi-Bidgoli A, Zarebanadkouki M. The potential impact of biochar: soil hydraulics and responses of maize under soil drying cycles. *Geoderma*, 2021, **401**: 115301
40. Fernandes R D M, Egea G, Hernandez-Santana V, Diaz-Espejo A, Fernández J E, Perez-Martin A, Cuevas M V. Response of vegetative and fruit growth to the soil volume wetted by irrigation in a super-high-density olive orchard. *Agricultural Water Management*, 2021, **258**: 107197
41. Kumar A, Sonkar I. Estimability analysis and optimization of soil hydraulic and abiotic stress parameters from root zone salt-water dynamics in soil column lysimeter. *Plant and Soil*, 2025, **513**(1): 107–136
42. Mao J, Wu J W, Liu Y W, Guo C Y, Xiao C N, Lu Y, Zhao L Y, Zhang R J, Zhang H Y. A model for simulating evaporation from seasonally frozen saline soil. *Journal of Hydrology*, 2025, **659**: 133259
43. Luo P C, Zhao L, Chen R, Chen P P, Dhital Y P, Li H Q, Wang D W, Yang J J, Chen Y, Liu Q G, Wang Z H. Leaching salinity and mulching straws during freeze-thaw period enhance post-thawing cotton yield and quality by optimizing soil aggregates stability. *Soil and Tillage Research*, 2025, **250**: 106506
44. Naghedifar S M, Ziaei A N, Ansari H. Simulation of irrigation return flow from a *Triticale* farm under sprinkler and furrow irrigation systems using experimental data: a case study in arid region. *Agricultural Water Management*, 2018, **210**: 185–197
45. Qi D L, Hu T T, Song X. Effects of nitrogen application rates and irrigation regimes on grain yield and water use efficiency of maize under alternate partial root-zone irrigation. *Journal of Integrative Agriculture*, 2020, **19**(11): 2792–2806
46. Guo K, Feng X H, Liu X J, Ju Z Q. Long-term freezing saline water irrigation and cotton cultivation improved soil properties and maintained low salinity in the root zone of coastal saline soil. *Soil Use and Management*, 2024, **40**(4): e13117
47. Abd-Elaty I, Ramadan E M, Elbagory I A, Nosair A M, Kuriqi A, Garrote L, Ahmed A A. Optimizing irrigation systems for water efficiency and groundwater sustainability in the coastal Nile Delta. *Agricultural Water Management*, 2024, **304**: 109064
48. Liu B X, Wang S Q, Liu X J, Sun H Y. Evaluating soil water and salt transport in response to varied rainfall events and hydrological years under brackish water irrigation in the North China Plain. *Geoderma*, 2022, **422**: 115954
49. Yan S H, Zhang T B, Zhang B B, Feng H. A revised saline water quality assessment method considering including Mg^{2+}/Na^{+} as a new indicator for an arid irrigated area. *Journal of Hydrology*, 2024, **639**: 131619
50. Du L, Zheng Z C, Li T X, Zhang X Z. Effects of irrigation frequency on transportation and accumulation regularity of greenhouse soil salt during different growth stages of pepper. *Scientia Horticulturae*, 2019, **256**: 108568
51. Barnard J H, van Rensburg L D, Bennie A T P. Leaching irrigated saline sandy to sandy loam apedal soils with water of a constant salinity. *Irrigation Science*, 2010, **28**(2): 191–201
52. Li Z J, Liu H G, Wang T G, Gong P, Li P F, Li L, Bai Z T. Deep vertical rotary tillage depths improved soil conditions and cotton yield for saline farmland in south Xinjiang. *European Journal of Agronomy*, 2024, **156**: 127166
53. Zhu W, Yang J S, Yao R J, Wang X P, Xie W P, Shi Z G. Buried layers change soil water flow and solute transport from the Yellow River Delta, China. *Journal of Soils and Sediments*, 2021, **21**(4): 1598–1608
54. Berezniak A, Ben-Gal A, Mishael Y, Nachshon U. Manipulation of soil texture to remove salts from a drip-irrigated root zone. *Vadose Zone Journal*, 2018, **17**(1): 1–11
55. Dong S D, Wang G M, Kang Y H, Ma Q, Wan S Q. Soil water and salinity dynamics under the improved drip-irrigation scheduling for ecological restoration in the saline area of Yellow River basin. *Agricultural Water Management*, 2022, **264**: 107255
56. Zhang Y, Liu H G, Gong P, He X L, Wang J X, Wang Z L, Zhang J R. Irrigation method and volume for Korla fragrant pear: impact on soil water and salinity, yield, and fruit quality. *Agronomy*, 2022, **12**(8): 1980
57. Chen W L, Jin M G, Ferré T P A, Liu Y F, Xian Y, Shan T R, Ping X. Spatial distribution of soil moisture, soil salinity, and root density beneath a cotton field under mulched drip irrigation with brackish and fresh water. *Field Crops Research*, 2018, **215**: 207–221
58. Zhu W D, Li X B, Dong S D, Kang Y H, Cui G X, Miao J X, Li E Z. Planting trees in saline soil using ridge cultivation with drip irrigation in an arid region of China. *Land Degradation & Development*, 2022, **33**(8): 1184–1192